

# Stable crack growth in ductile polymers

S. BAZHENOV

*Institute of Chemical Physics, Kosygin Street 4, 117977 Moscow, Russia*

Growth of a crack in ductile polymers (polyarylate, PTFE, and PU/PMMA blends) was studied. The crack growth was described assuming that local yielding in the crack tip is similar to large-scale shear yielding in rigid-plastic materials. Crack growth was stable, and a wedge shaped crack tip was formed. The crack tip opening displacement and the crack extension in the initial stage of the crack growth were proportional to the square of the strain up to 11% elongation. Dugdale's equation was modified to describe the magnitude of the crack tip opening. In PA, a yield subzone near the crack tip was observed.

## 1. Introduction

Failure in the presence of stress concentrators has been intensively studied for a long time. As a result, clear theoretical foundations of failure have been developed for two contrasting cases. The first is that of brittle materials for which the Griffith's energy criterion describes the stress at crack initiation [1]. Clear theory has been developed also for the opposite case of rigid-plastic materials where crack growth is caused by large-scale yielding [2–4] leading to the formation of a wedge-shaped crack tip. The angle of the wedge is equal to  $90^\circ$  for plane strain and to  $70^\circ 32'$  for plane stress conditions [3].

Polymers are usually neither ideally brittle nor ideally ductile, and their properties are intermediate to these two extreme cases. Griffith's theory of brittle fracture is usually used as a foundation, and efforts are directed to its modification in order to consider material ductility. Modification of Griffith's fracture theory was successful for quasibrittle materials where yielding is limited to a small volume near the fracture surfaces [5, 6]. In less-brittle materials, stable "sub-critical" crack growth is often observed, and linear elastic fracture mechanics fails to explain it. In this work ductile polymers were studied, and ductility theory was combined with Dugdale's model [7] to describe an initial stable stage of the crack growth.

The aim of the work was to study stable crack growth in ductile polymers, Young's modulus and the ability to strain-harden of which vary over a wide range.

## 2. Experimental procedure

### 2.1. Materials

Five ductile polymers with Young's modulus varying from rubber-like ( $\approx 0.1$  GPa) to  $\approx 2$  GPa were tested. These polymers were polyarylate (PA), polytetrafluoroethylene (PTFE), and three polyurethane/polymethacrylate (PU/PMMA) blends with 70/30, 50/50, and 20/80 PU/PMMA ratios by weight. In PU/PMMA blends MMA monomer polymerization preceded curing of polyurethane gel.

### 2.2. Tests procedure

Specimens were rectangular films, 30 mm long and 10 mm wide. The thickness of the test specimens was 60  $\mu\text{m}$  for PA, 180  $\mu\text{m}$  for PTFE and 1.2 mm for PU/PMMA blends. A short notch, 0.4–2 mm long, was made on one edge of each specimen (Fig. 1). Mechanical tests were performed in tension at room temperature with a minitest machine made for use with an optical microscope. The crosshead speed was low, 0.01  $\text{mm min}^{-1}$  for PA and 0.05  $\text{mm min}^{-1}$  for the other four polymers. Unnotched specimens were tested with an "Instron 1169" test machine at a crosshead speed of 0.2  $\text{mm min}^{-1}$  according to the ASTM procedure.

During testing with the minitest machine, a load–displacement curve was automatically recorded, and the crack tip was periodically photographed with a camera. After the onset of crack growth, a wedge-shaped crack tip was formed. The crack tip opening displacement,  $\delta$ , and the crack extension,  $\Delta L$ , were measured using negatives with a low-magnification optical microscope, as illustrated Fig. 1. The crack tip opening displacement and the crack extension were not determined if  $\delta$  was less than 15  $\mu\text{m}$  and the wedge was not formed. The angle of the crack tip wedge,  $\phi$  was calculated assuming a triangular shape of the wedge

$$\phi = 2 \arctan \frac{\delta}{2\Delta L} \quad (1)$$

where  $\delta$  is the crack tip opening displacement and  $\Delta L$  is the crack extension.

Stress in notched specimens was calculated as  $P/(S_0 - S_c)$ , where  $P$  is the applied load,  $S_0$  and  $S_c$  are the cross-sectional areas of the unnotched specimen and the initial notch length. Decrease in the cross-sectional area caused by growth of the crack was not taken into account. Strain was calculated as the ratio of the grip displacement to the specimen length.

## 3. Results

### 3.1. Mechanical properties

Fig. 2 shows engineering stress–strain curves for unnotched polymers. All polymers are ductile and the

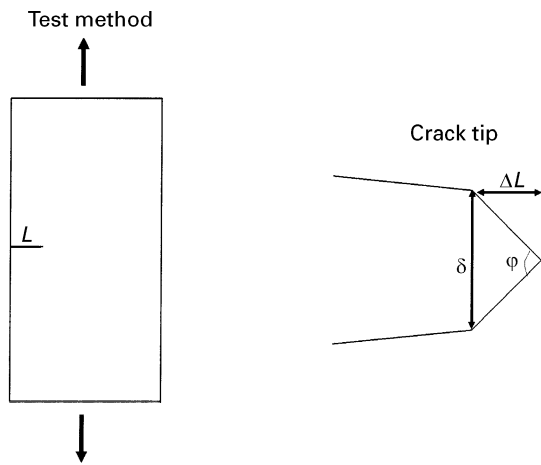


Figure 1 The edge-notch tensile test.

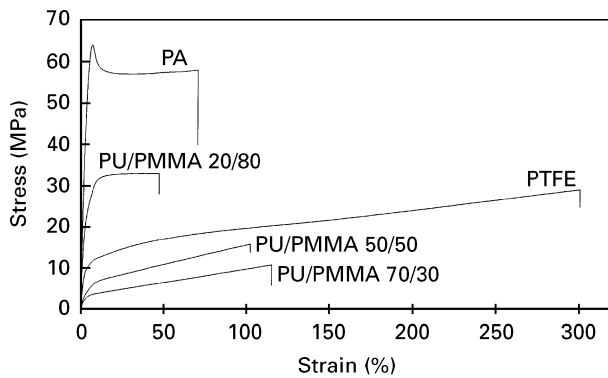


Figure 2 Engineering stress plotted against strain for PA, PU/PMMA 20/80 blend, PTFE (3), PU/PMMA 50/50, and 70/30 blends.

TABLE I Mechanical properties

Polymer	Modulus (MPa)	Yield stress (MPa)	Strength (MPa)
PA	1730	64	60
PTFE	450	11.3	29
PU/PMMA 20/80	960	32	33
PU/PMMA 50/50	155	5.5	16
PU/PMMA 70/30	110	3.5	12

fracture strain exceeded 50%. The Young's modulus varies from  $\approx 0.1$  to 1.7 GPa and the yield stress varies from 3.5 to 64 MPa. PA (curve 1) yields with necking, resulting in the maximum on the stress–strain curve, and the other four polymers yield uniformly without necking. Mechanical properties of the polymers are presented in Table I.

Fig. 3 shows typical stress–strain curves for notched PA and PU/PMMA 70/30 blend, polymers with the highest and the lowest Young's moduli. Arrows indicate the points where the crack growth was noticed. The strain of the crack initiation depends on the notch length. In rigid PA, the crack growth was initiated at a strain of 0.8%–1.4% depending on the notch length. The stress–strain relationship at these strains is linear. The start of the crack resulted in the appearance of a non-linearity in the stress–strain curve. Stable crack

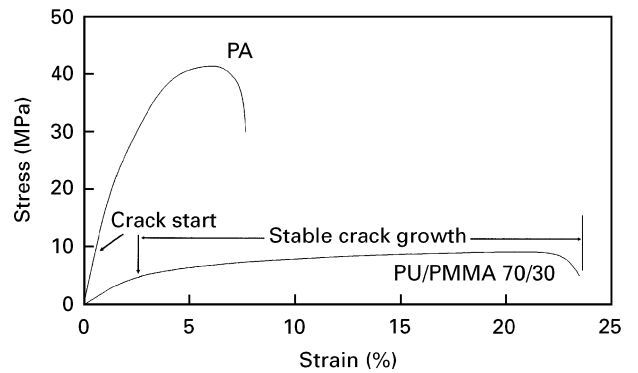


Figure 3 Engineering stress plotted against strain for notched PA, and PU/PMMA 70/30 blend.

growth was followed by catastrophic fracture of PA at a strain of 5%–7%. The crack in the soft PU/PMMA 70/30 blend started at strains of 2%–4.5%. The shortest cracks in this blend initiated after the onset of large-scale yielding, and their growth was stable up to 25% strain. The transition to unstable fracture was observed in PA and PU/PMMA 20/80 blend, while in other polymers the crack growth was stable after the stress maximum point.

### 3.2. Yield zone

Fig. 4a shows the crack in PA in polarized light at a strain of  $\varepsilon = 0.8\%$ , immediately before onset of the crack growth. In front of the crack, a dark circular yield zone with an  $\varepsilon$ -shaped stress concentration region is observed. Two dark lines in the  $\varepsilon$ -shaped region, oriented at an angle of  $57^\circ$ – $58^\circ$  to the crack plane, correspond to the direction of the highest shear stress concentration. The pole of the elastic stress concentration regions is close to the tip of the plastic zone.

Fig. 4b shows the growing crack at higher strain. The yield zone is elongated; in the vertical position the yield zone looks like a candle flame. The crack tip has a wedge shape with an angle of  $\approx 55^\circ$ . Further loading leads to a decrease in the wedge angle (Fig. 4c). The arrow in Fig. 4c indicates the diffuse dark zone in the crack tip that moves with it (Fig. 4d and e). The zone is oriented at an angle of  $66^\circ$ – $69^\circ$  to the crack plane. The dark colour of this zone reflects the higher orientation of the polymer in it. Thus, a strain distribution in the yield zone is not uniform, and in the tip of the growing crack a “yield subzone” is observed. A schematic drawing of the crack tip zone in PA is presented in Fig. 5. In all polymers the crack tip had the wedge shape, the angle of which varied from  $25^\circ$  to  $120^\circ$ .

The stress intensity factor,  $K_I$ , for an edge notch is given by Equation [8]

$$K_I = Y\sigma L^{1/2} \quad (2)$$

where  $\sigma$  is the applied stress,  $L$  is the initial crack length. For an edge notch  $Y = 1.99 - 0.41\lambda + 18.70\lambda^2 - 38.48\lambda^3 + 53.85\lambda^4$ , where  $\lambda = L/w$ , and  $w$  is the specimen width.

Fig. 6 shows the crack resistance  $J = K_I^2/E$  plotted against crack extension,  $\Delta L$ , for PU/PMMA 50/50

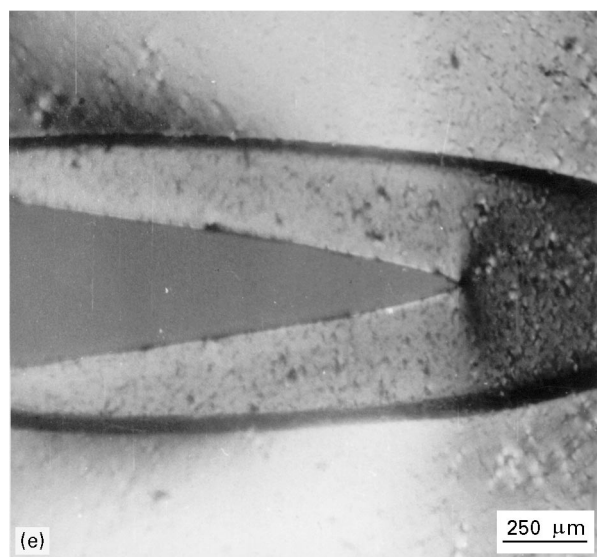
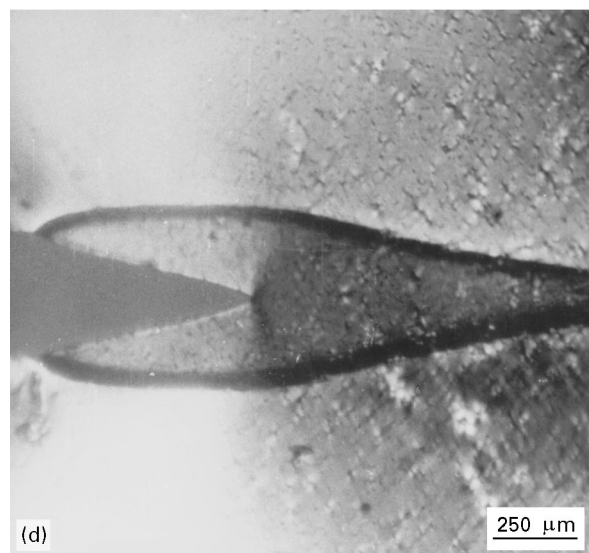
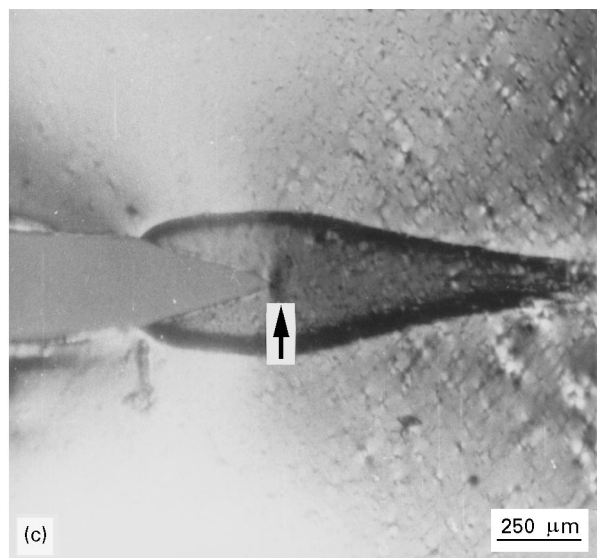
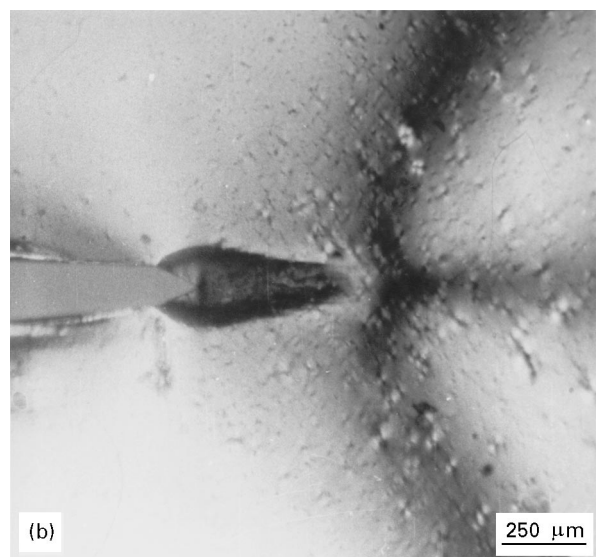
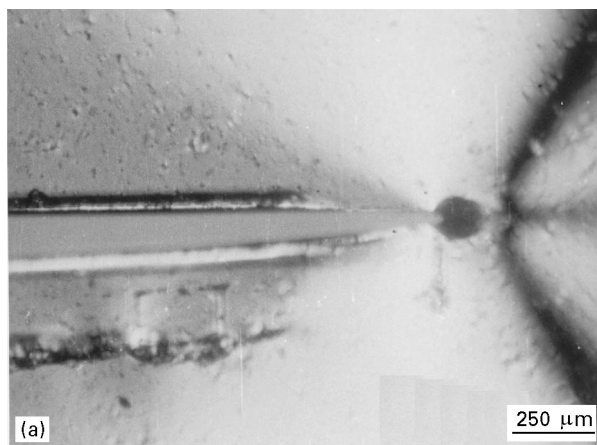


Figure 4 Transmission optical micrographs of a growing crack in PA: polarized light.

blend at different initial crack lengths. The  $J$ - $\Delta L$  relationship is not described by a single curve, and hence the energy approach cannot be used to describe the crack growth in this blend. This may be attributed to the ductility of the polymer.

### 3.3. Model

Stress concentration near a crack in quasibrittle materials is usually described on the basis of

Griffith–Orowan’s theory of brittle fracture. Local plasticity in this case is considered by introduction of an effective fracture toughness [5,6]. However, for ductile polymers, the ductility theory may be a more suitable foundation than linear elastic fracture mechanics.

The presence of a local yield subzone allows introduction of a model which approximates yielding in the crack tip by large-scale shear yielding in rigid-plastic materials, Fig. 7. According to plasticity theory, yielding near an edge notch is by shear in a network of lines oriented at an angle of  $45^\circ$  to the load direction for plane strain and at an angle of  $\approx 55^\circ$  for plane stress conditions.

Fig. 8 shows schematically the formation mechanism of the wedge in the crack tip by alternative shear slip along yield lines. The angle of the crack tip wedge,  $\varphi$ , is equal to the angle between the slip lines

$$\varphi = \theta \quad (3)$$

where  $\theta$  is the angle between the yield lines.

For plane strain conditions,  $\varphi$  is equal to  $90^\circ$ , and according to Equation 1 the crack length increment,

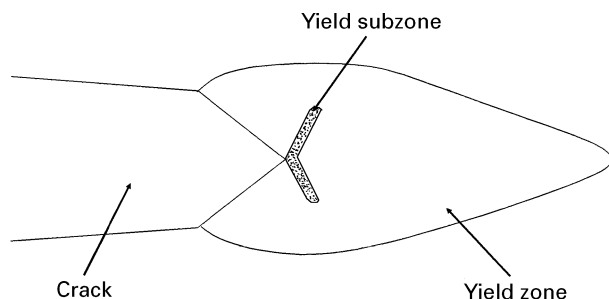


Figure 5 Schematic drawing of the crack tip zone in PA.

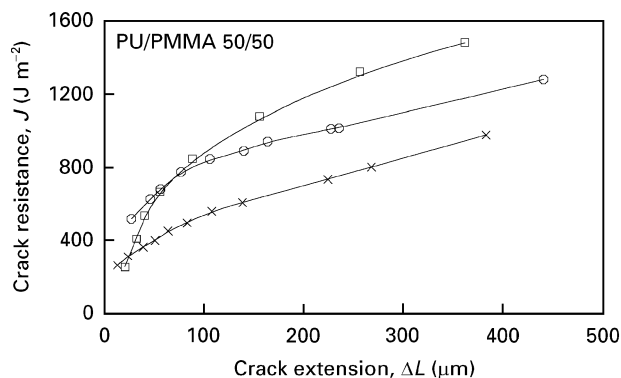


Figure 6 The crack resistance,  $J$ , plotted against crack extension,  $\Delta L$ , for PU/PMMA 50/50 blend. Initial crack length,  $L$ : ( $\times$ ) 0.46 mm, ( $\circ$ ) 1.06 mm and ( $\square$ ) 1.86 mm.

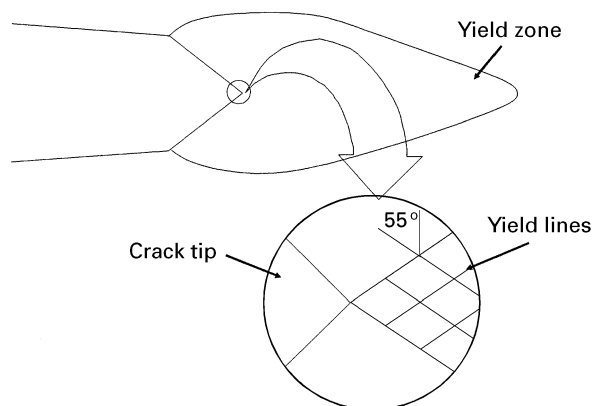


Figure 7 Model describing yield in the crack tip.

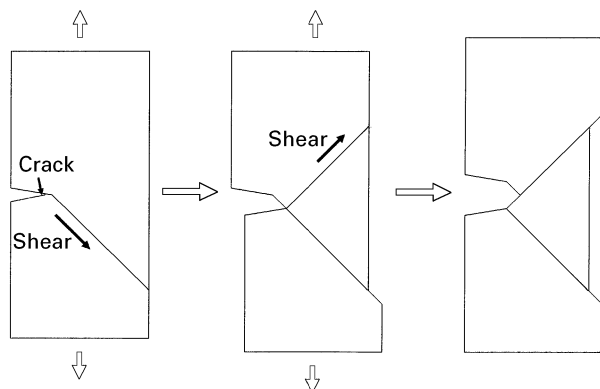


Figure 8 Schematic illustration of the formation mechanism of a crack wedge by alternative slips in two sets of yield lines.

$\Delta L$ , should be equal to  $\delta/2$ . Similarly, for plane stress  $\varphi = 2 \arctan(1/2^{1/2})$ , and  $\Delta L = \delta/2^{1/2}$ . In both cases the crack extension is determined by the crack tip opening displacement.

### 3.4. Crack tip opening displacement

At low strains in elastic-plastic materials, the crack tip opening displacement is given by Dugdale's equation [7]

$$\delta = \frac{K_I^2}{E\sigma_0} = \frac{Y^2\sigma^2L}{E\sigma_0} \quad (4)$$

where  $\sigma$  is the applied stress,  $\sigma_0$  is the yield stress, and  $E$  is the Young's modulus of the polymer.

According to Equation 4 the crack tip opening displacement,  $\delta$ , should be proportional to  $Y^2\sigma^2L$ . Experimental data show that for PU/PMMA blends,  $\delta$  is not proportional to the square of stress and, in addition, the  $\delta - Y^2\sigma^2L$  relationship is not described by a single curve if the crack length is changed. For this reason, Dugdale's equation was modified to describe the experimental data.

Linear elastic fracture mechanics describes fracture in terms of stress, energy and Young's modulus. In contrast, plasticity theory operates with displacements and strains. For this reason, an attempt was made to use strain instead of stress. Stress in the linear elastic region is proportional to strain, and Equation 4 may be rewritten

$$\delta = \frac{Y^2\varepsilon^2LE}{\sigma_0} \quad (5)$$

Fig. 9a shows the crack tip opening displacement,  $\delta$ , plotted against  $Y^2\varepsilon^2L$  for PU/PMMA 50/50 blend. Fig. 9b shows that the initial part of the curve in

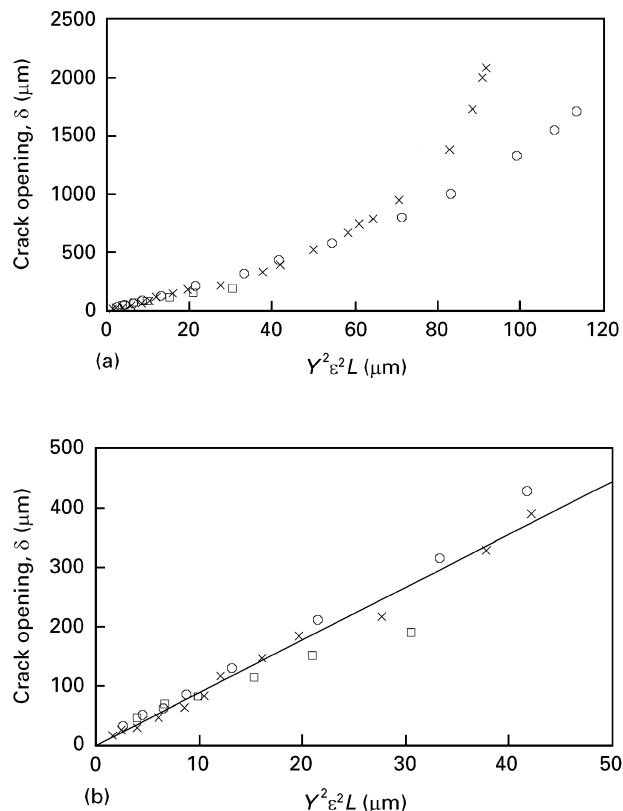


Figure 9 (a) The crack tip opening,  $\delta$ , plotted against  $Y^2\varepsilon^2L$  for PU/PMMA 50/50 blend. (b) The initial linear part of the curve.  $L$ : ( $\times$ ) 0.46 mm, ( $\square$ ) 1.06 mm, ( $\circ$ ) 1.86 mm.

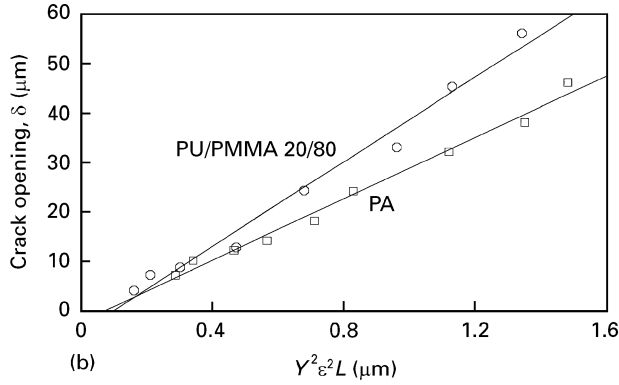
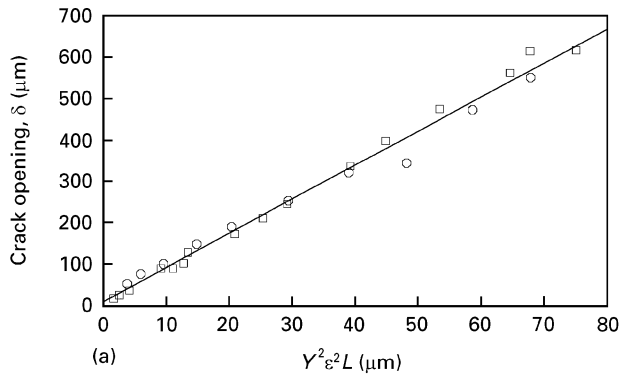


Figure 10 Initial linear part of  $\delta$  versus  $Y^2\epsilon^2L$  curves for (a) PU/PMMA 70/30 blend and (b) PU/PMMA 20/80 blend and PA.  $L$ : (○) 1.03 mm, (□) 0.49, (—) best fit.

Fig. 9a is linear, in agreement with Equation 5. At higher strains, the dependence in Fig. 9a is not linear and is not described by a single curve at different notch lengths. Fig. 10 shows that the initial parts of  $\delta$ - $Y^2\epsilon^2L$  curves are linear for PU/PMMA 70/30 blend (Fig. 10a), PU/PMMA 20/80 blend, and PA (Fig. 10b). It is worth mentioning that for PU/PMMA 50/50 blend (Fig. 9b),  $\delta$  is proportional to  $\epsilon^2$  up to strain of  $\epsilon = 11.4\%$  at crack length  $L = 0.46$  mm. At crack length  $L = 1.86$  mm, the proportionality is observed up to  $\epsilon = 4.6\%$ .

Increase of the crack tip opening displacement,  $\delta$ , in proportion to  $\epsilon^2$  is not surprising at low strains ( $\epsilon < 3\%$ ) when assumptions of Dugdale's equation are fulfilled. However,  $\delta$  is proportional to  $\epsilon^2$  even when a polymer has undergone general yield, far beyond the area of validity of Dugdale's equation. The reason is not clear.

For analysis of the quantitative applicability of Equation 5, the parameter  $\sigma_0$  is considered. In Dugdale's equation,  $\sigma_0$  is the yield stress of the polymer. The experimental value of  $\sigma_0$  was calculated from Young's modulus and the slopes of the straight lines in Figs 9b and 10. Fig. 11 shows the ratio of calculated  $\sigma_0$  value to the yield stress,  $\sigma_0/\sigma_y$ , plotted against yield stress,  $\sigma_y$ . Similarly, Fig. 12 shows the ratio of calculated  $\sigma_0$  values to the strength limit,  $\sigma_0/\sigma_t$ , plotted against  $\sigma_t$ . For all polymers, the calculated  $\sigma_0$  value is close to the polymer strength,  $\sigma_t$ . Thus,  $\sigma_0$  is equal to the engineering fracture stress in Equation 5 and describes the magnitude of crack opening better than the yield stress. For a central crack in an

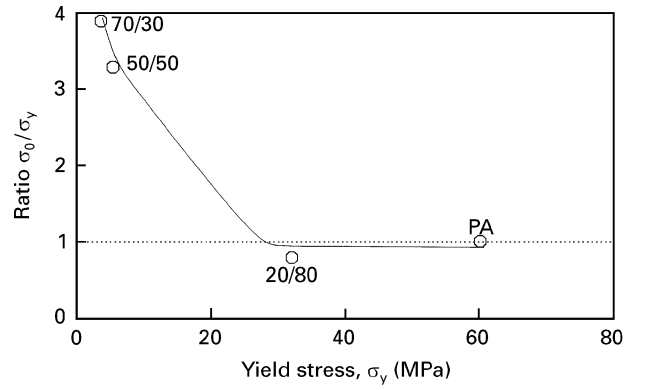


Figure 11  $\sigma_0/\sigma_y$  ratio plotted against the yield stress,  $\sigma_y$ .

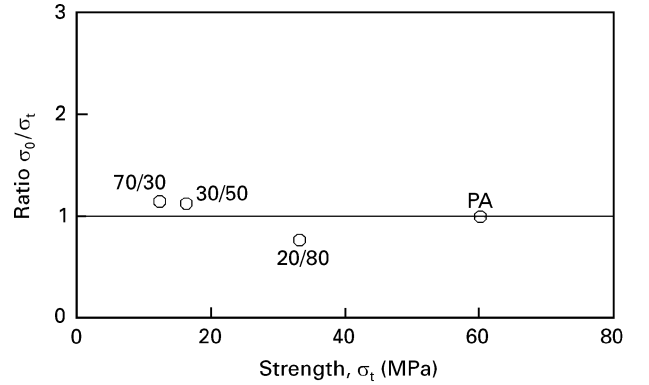


Figure 12  $\sigma_0/\sigma_t$  ratio plotted against polymer strength,  $\sigma_t$ .

infinite plate,  $Y^2 = \pi$  [8], and Equation 5 may be rewritten

$$\delta = \frac{\pi\epsilon^2LE}{\sigma_t} \quad (6)$$

where  $\sigma_t$  is the strength of an unnotched polymer.

### 3.5. Crack extension

Tested specimens were thin and hence are in plane stress conditions. According to the above model, crack extension for plane stress is given by

$$\Delta L = \frac{Y^2\epsilon^2LE}{2^{1/2}\sigma_t} \quad (7)$$

For plane strain,  $\Delta L$  is given by

$$\Delta L = \frac{Y^2\epsilon^2LE}{2\sigma_t} \quad (8)$$

Fig. 13 shows the crack extension,  $\Delta L$ , plotted against the crack opening,  $\delta$ , for the five polymers studied. The agreement of experimental data with the model prediction (thin straight line) is satisfactory for PTFE, PU/PMMA 50/50, and PU/PMMA 70/30 blends. For PA and PU/PMMA 20/80 blend, the agreement is good only after onset of the crack growth. Further crack growth leads to a transition to quasibrittle fracture and essential disagreement with the model prediction.

Fig. 14 shows the angle of the crack tip wedge,  $\phi$ , plotted against the crack opening,  $\delta$ . Some decrease in

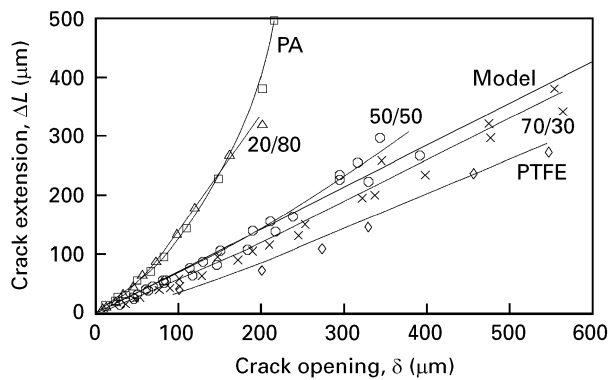


Figure 13 The crack extension,  $\Delta L$ , plotted against the crack tip opening,  $\delta$ , for (□) PA, and PU/PMMA (Δ) 20/80, (○) 50/50, (×) 70/30 blends, and (◇) PTFE. (—) Model.

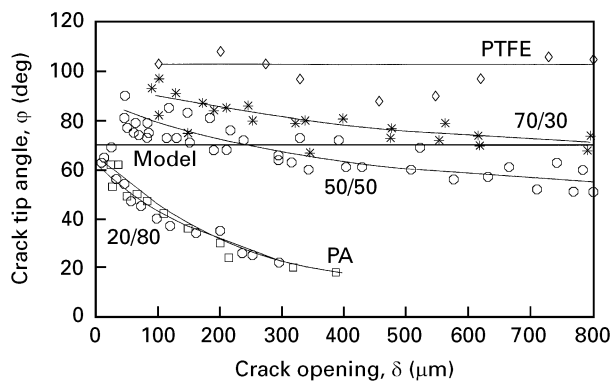


Figure 14 Crack tip angle,  $\phi$ , plotted against the crack opening,  $\delta$ , for PA, and PU/PMMA 20/80, 50/50, 70/30 blends, and PTFE. The thin straight line describes the model prediction  $\phi \approx 70^\circ$  for the plane stress condition.

$\phi$  with crack opening is observed for all polymers, except for PTFE where  $\phi$  is practically constant. The decrease in  $\phi$  is especially significant in rigid PA and PU/PMMA 20/80 blend, where it precedes a transition to unstable fracture. The agreement of the model prediction  $\phi = 70^\circ$  with experimental data is comparatively good for PU/PMMA 50/50 and 70/30 blends. For PTFE, the experimental  $\phi$  value is somewhat higher than the theoretical value. This may be explained by essential strain-hardening of the polymer which leads to an increase in  $\phi$  values [9]. For PA and PU/PMMA 20/80 blend, the agreement is good only after onset of the crack growth. Further crack growth leads to sharpening of the crack tip wedge due to transition to quasibrittle fracture.

Fig. 15 shows the initial parts of crack extension,  $\Delta L$ , versus  $Y^2 \varepsilon^2 L$  curves ( $\Delta L < 160 \mu\text{m}$ ). Lines describe theoretical dependencies (Equation 7). Crack extension increases proportionally to  $\varepsilon^2$ , and agreement of experimental data with Equation 7 is satisfactory. For quasibrittle PA and PU/PMMA 20/80 blend crack wedge sharpening leads to disagreement with the model predictions.

#### 4. Discussion

The stress concentration near a crack is usually considered on the basis of linear elastic fracture

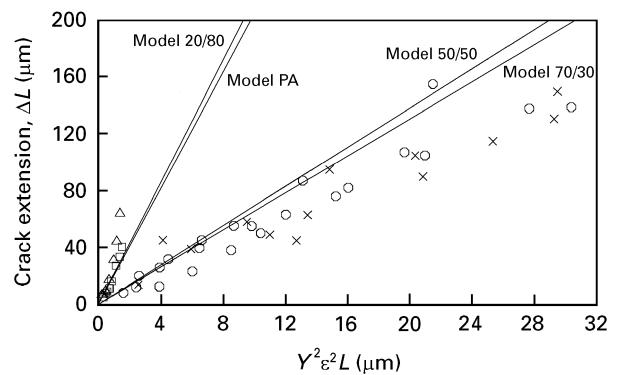


Figure 15 The crack extension,  $\Delta L$ , plotted against  $Y^2 \varepsilon^2 L$  factor for (○) PU/PMMA 50/50 blend, (×) PU/PMMA 70/30 blend, (□) PA, and (Δ) PU/PMMA 20/80 blend. The straight line describes the model predictions.

mechanics. However, stable crack growth may also be considered by combination of plasticity theory with modified Dugdale's solution for crack opening. This approach explains the wedge shape of a crack tip and the stable mechanism of crack growth. In addition, it approximately describes the magnitude of the crack tip opening and the crack extension on the initial stage of the crack growth. At the same time, this approach does not explain the cause of some sharpening of the growing crack.

#### 5. Conclusions

1. The initial stage of crack growth is described assuming that local yielding in the crack tip is similar to large-scale yielding in rigid-plastic materials.
2. The crack tip opening displacement increases proportionally to the square of strain, even after onset of large-scale yielding.
3. In PA, a yield subzone near the crack tip was observed.

#### Acknowledgements

The author thanks Dr A. Liapunov and Dr N. S. Grineva for technical help and supply of polymers, and Professor L. I. Manevich for stimulating discussions.

#### References

1. A. A. GRIFFITH, *Phil. Trans. R. Soc. Ser. A* **221** (1920) 163.
2. L. M. KACHANOV, "Plasticity theory" (Nauka, Moscow, 1969).
3. F. A. McCLINTOCK, in "Fracture", edited by H. Liebowitz, Vol. 3 (Academic Press, New York, 1971) p. 66.
4. C. F. SHIH, H. G. DE LORENZI, W. R. ANDREWS, R. H. VAN STONE, J. P. D. WILKINSON, "Methodology for plastic fracture", Report by General Electric Co., June 1977.
5. E. OROWAN, *Welding Res. Suppl.* **20** (1955) 1575.
6. G. R. IRWIN, "Fracture dynamics, Fracturing of Metals" (ASM, Cleveland, OH, 1948) p. 147.
7. D. S. DUGDALE, *J. Mech. Phys. Solids* **8** (1960) 100.
8. V. Z. PARTON and E. M. MOROZOV, "Mechanics of elastic-plastic fracture", 2nd Edn (Edition of Physical-Mathematical Literature, Moscow, 1985) p. 502.
9. J. W. HUTCHINSON, *J. Mech. Phys. Solids* **16** (1968) 13.

Received 22 December 1994  
and accepted 2 July 1996